STUDIES ON PEROVSKITE BASED HETEROJUNCTION SYSTEMS FOR PHOTOELECTROCHEMICAL SPLITTING OF WATER

Synopsis

Submitted in the partial fulfilment for the requirement of

Doctor of Philosophy

in

CHEMISTRY

Submitted by

ANUSHTHA BHARDWAJ

Under the supervision of

Dr. Saritha. A
Co-Supervisor
Associate Professor
Department of Chemistry
Amrita Vishwavidyapeetham University
Amritapuri, Kollam

Dr. Manju Srivastava
Supervisor
Assistant Professor

Department of Chemistry, Faculty of Science
Dayalbagh Educational Institute (Deemed to be University)
Dayalbagh, Agra-282005
2024

1. Solar energy driven water splitting in photoelectrochemical (PEC) cell

1.1 Importance of the proposed work

The extensive use of conventional fossil fuels and the resulting environmental degradation have become significant hindrances to global sustainable growth. As per a United Nations (UN) report, the global population is projected to reach 9.8 billion by 2050, while the BP Statistical Review of World Energy in 2020 indicates that carbon-emitting sources account for over 60% of the world's energy supply (Aghakhani et al., 2023).

Currently, the world's energy needs are met through a mix of energy production methods, including nuclear and hydrothermal (13%), fossil fuels (57%), and renewables (30%) (Kulshreshtra et al., 2023). Historically, fossil fuels have been the primary contributors to this energy supply due to their affordability. However, their excessive consumption has led to resource depletion, climate change, increased greenhouse gas emissions, global warming, and hindered economic growth (Saraswat et al.,2018).

Internationally, several initiatives have been implemented to mitigate these issues, including the Paris Agreement, the Kyoto Protocol, and Conference of the Parties (COP26). India, for instance, committed to achieving carbon neutrality by 2070 in Conference of the Parties COP26, as part of a five-point action plan that involves a net-zero emissions target by 2070 and a 50% reduction in emissions by 2030. To address the energy demand while mitigating climate change, renewable energy resources are seen as a more sustainable, reliable, and cost-effective alternative today. Currently, 14% of the world's total energy demand is met by renewable sources like biomass, hydropower, geothermal, solar, wind, and marine energy.

However, these renewable energy sources have their limitations, including low energy density, high setup costs, and storage challenges. Analyzing unit energy costs reveals that using these methods for energy generation is not always economical. To address these challenges, two key renewable energy sources, solar energy, and water, have shown promise in producing a future green fuel, hydrogen, through water splitting.

Hydrogen can be produced using various methods depending on renewable sources like wind, solar, geothermal, biomass, and non-renewable sources such as fossil fuels (e.g., coal and natural gas). While

hydrogen production from fossil fuels has historically been a major contributor, it also leads to the generation of toxic byproducts.

Solar energy has become a preferred choice because it is the most abundant of all non-renewable and renewable resources. The solar energy reaching Earth (173,000 TW) is nearly 9600 times larger than the daily total global energy consumption (17.91 TW in 2017). Approximately 54% of the electromagnetic radiation released falls within the ultraviolet and visible range, providing clean and cost-effective energy. However, its effectiveness depends on geographical variations, weather conditions, and time of day (Koyale et al., 2023, Saraswat et al., 2018).

Hydrogen, as a green fuel, is an attractive option due to its non-toxic nature, lack of byproducts, optimal combustion efficiency, and significant energy density. It is predicted to reduce dependence on fossil fuel-based energy resources.

Green hydrogen can be generated through various methods such as photobiological, photocatalytic, electrocatalytic, photovoltaic (PV), and photoelectrochemical (PEC). Photoelectrochemical (PEC) has emerged as a key approach for hydrogen production from abundant renewable resources due to its advantages over alternative techniques. Photoelectrochemical (PEC) technology is based on a single cell arrangement where a semiconductor electrode absorbs sunlight to split water into H_2 and O_2 without generating any hazardous byproducts. It also aligns with an economical, large-scale manufacturing strategy.

In contrast, other methods like photovoltaic (PV) and electrocatalytic require external energy to split water and face high-cost management and energy storage challenges. Photobiological methods rely on the activity of microbes to absorb solar energy for H_2 production, resulting in low production at high costs, limiting scalability. Photocatalytic methods face limitations in separating produced H_2 and O_2 due to shared electrodes.

In summary, this work is focused on Photoelectrochemical (PEC)water splitting for hydrogen generation, initially demonstrated in 1972 by Fujishima and Honda using single-crystalline TiO_2 (rutile) as an anode and a Pt cathode under ultraviolet (UV) irradiation with an applied external bias. However, the challenge remains in efficiently producing hydrogen through the photoelectrochemical (PEC) route. The proposed work aims to create a stable, visible-light-absorbing photoelectrode that is robust and less

toxic to achieve the mentioned goals.

1.2 Brief Description of photoelectrochemical (PEC) Mechanism

In a photoelectrochemical (PEC) cell, a semiconductor material is immersed in an electrolyte, creating a solid-liquid junction. This junction combines a photoelectrode with a counter electrode within an electrolytic solution, bridged by an external bias equal to or greater than 1.23 V. The functioning of this cell involves the following components:

- **Photoelectrode (working electrode):** This element is constructed from a semiconductor material with an appropriate band gap.
- **Counter electrode:** Typically made of metal, such as platinum (Pt), it pairs with the working electrode to complete the electrical circuit.
- **Electrolyte:** This component serves as the medium for the redox reaction to occur.

The crucial element, the photoelectrode, is composed of a semiconductor material layered on a conductive substrate like tin-doped indium oxide (In_2O_3: Sn, ITO) or fluorine-doped tin oxide (FTO). The specific nature of the semiconductor material dictates how the cell operates in the redox reaction. Semiconductors are classified into two categories: n-type and p-type semiconductors, and their arrangements within the cell are as follows:

- **n/p-type Photoelectrode:** When an n-type or p-type photoelectrode is connected with a counter electrode (Pt) and immersed in an electrolyte solution, it drives the cell's activity.
- **n-type Photoelectrode with p-type Photoelectrode:** In this configuration, the n-type photoelectrode is connected to the p-type photoelectrode, creating a tandem cell. The cell's performance depends on the choice of the working electrode.

The latter configuration is an evolving setup capable of providing a self-sufficient and stand-alone cell design. Meanwhile, the former represents the primary arrangement, elucidating the fundamental operation of the photoelectrochemical (PEC) cell, as illustrated in the accompanying figure 1.

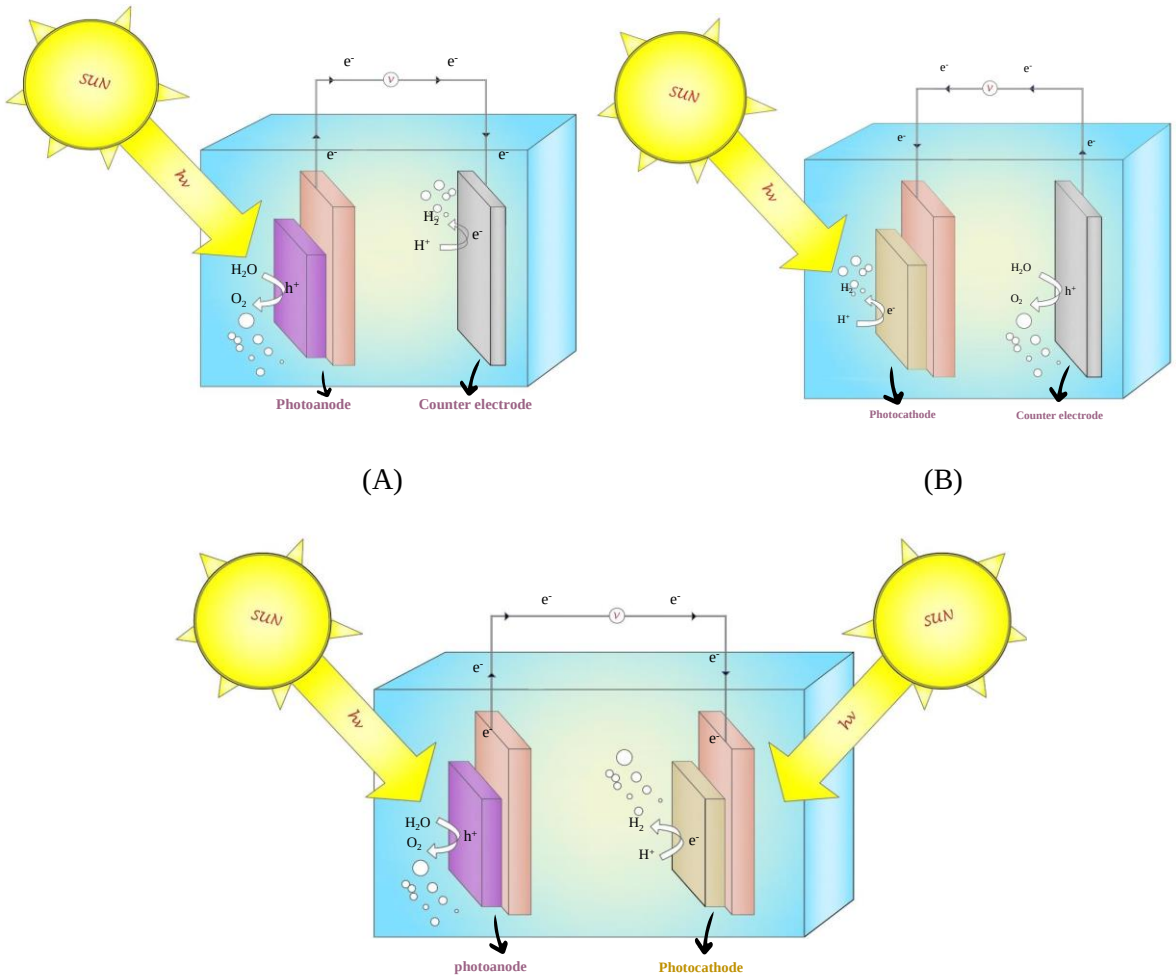

(A) (B)

(C)

Figure 1 (A) represents the n-type working electrode as photoanode liberates H_2 at counter electrode, (B) represents p-type working electrode as photocathode liberates H_2 at same electrode while (C) shows tandem cell working, liberation of H_2 at photocathode.

1.2.1 Semiconductor requirements

The production of green hydrogen through photoelectrochemical water splitting is critically reliant on the properties of the semiconductor material used in the photoelectrode. An ideal photoelectrode must meet specific criteria to ensure efficient photocatalytic activity. These requirements are outlined below (Luo et al.,2019; Tao et al.,2019; Tayebi et al.,2019; Wang et al.,2019; Dong et al.,2023; Kurnia et al.,2023; Chen et al.,2021; Gou et al.,2021)

a) Maximum Absorption of Visible Light: The photoelectrode should absorb a significant portion of the solar spectrum, especially within the visible light range.

b) Effective Charge Carrier Separation: It should efficiently separate generated charge carriers and facilitate their transport.

c) Appropriate Bandgap: The bandgap of the semiconductor material should fall within the range of 1.5-2.5 eV.

d) Positioned Band Edges: The band edges should straddle between the potential for water oxidation and reduction, with the conduction band (CB) being negative and the valence band (VB) being positive.

e) Low Overpotential: The photoelectrode should require minimal overpotential for the hydrogen and oxygen evolution reactions.

f) Surface Catalytic Activity: It should promote catalytic reactions on its surface.

g) Cost-Effective Production: The material should be cost-efficient to produce.

h) Chemical Stability: It must exhibit stability in both acidic and basic solutions.

i) Minimal Charge Carrier Losses: There should be reduced losses during the movement of charge carriers to the interface between the semiconductor and the electrolyte in the back contact.

Meeting these requirements is essential for the development of effective and sustainable photoelectrochemical systems for green hydrogen generation.

1.2.2 Working of photoelectrochemical (PEC) Mechanism

Sunlight illumination (greater than band gap of photoelectrode) generates the electron-hole pairs. The generated e^- transfers from the valence band (VB) to conduction band (CB) after leaving the holes in the valence band (VB). The electrons in the conduction band (CB) will be moved to conductive substrates before passing through an external circuit and arriving at the counter electrode connected with the supplied bias voltage for water reduction. Simultaneously, the holes in the valence band (VB) move towards the surface of the photoelectrode for water oxidation.

The overall water splitting of one mole of water into H_2 and O_2 (Eq. 3) involves two half - cell reactions i.e., for oxygen evolution followed generation of 4 equivalent of holes on oxidation while hydrogen evolution utilizes 2 electrons for reduction half - cell reaction (Eq.2)

Oxidation half - cell reaction

$2H_2O \rightarrow O_2(g) + 4H^+ + 4e^-$ $\quad E°_{oxi} = 1.23$ V Eq.1

Reduction half - cell reaction

$2H^+ + 2e^- \rightarrow H_2(g)$ $\quad E°_{red} = 0$ V Eq.2

Overall reaction

$2H_2O \rightarrow O_2(g) + 2H_2\ (g)$

2. Motivation

2.1 Challenging the Stability of Visible-Light Photoactive Materials

In the pursuit of harnessing solar energy for hydrogen generation, various materials, including metal oxides, metal sulfides, (Metal Organic Frameworks) MOFs, Covalent Organic Frameworks (COFs), Mxenes, and more, have been extensively explored for their suitability in capturing the visible spectrum of sunlight, which constitutes 2% of the ultraviolet (UV)-visible spectrum and a substantial 47% of the total solar light reaching the Earth's surface.

Semiconductor materials with narrow band gaps exhibit absorption in the visible region of the solar spectrum. However, their structural stability, electronic properties, and long-term efficiency have posed significant challenges, necessitating further investigation in the field of solar hydrogen generation. To address these challenges, the current focus is on the development of visible-light active photoelectrodes. This endeavor aims to mitigate impediments related to semiconductor materials, including issues like charge recombination, charge carrier diffusion length, electrode-electrolyte interface engineering, photo corrosion, and more.

To surmount these obstacles, innovative material design approaches will be employed, integrating modern modification techniques with straightforward preparation methods to enhance the stability and efficiency of visible-light photoactive materials.

3. Recent Literature Survey: A Concise Overview

The extensive literature studies on the materials (chalcogenides, perovskites, and perovskites- based metal oxides) for the application of photoelectrochemical studies with modifying material carbon-based structure are shown in table 1. While the table 2 shows the studies on MOFs (ZIF-8, ZIF-67) used as modification material for semiconductor material. The parameters studied range from modification performed, preparation method, and photoelectrochemical (PEC) observations, nature of photoelectrode etc. This whole survey describes the so far studies on these materials till now.

Table 1 Chalcogenides, perovskites, and perovskites-based metal oxides studies in photoelectrochemical studies

S.No.	Modification	Electrode/ Photo-electrode	Preparation Method	Observation	Lamp source	Electrolyte	Ref.
1.	R-GCN/Cu_3BiS_3	photocatalyst	Hydrothermal	increase in the photocurrent density	50 W LED lamp	-	Eslamluet. al 2023
2.	Cu_3BiS_3-$BiVO_4$Tandem	Photocathode-photoanode	Spray pyrolysis	Photocurrent density ~1.6 $mA.cm^{-2}$	50 W LED lamp	-	Eslamluet. al 2023
3.	Pt-Cu_3BiS_3	Photocathode	Spray pyrolysis	<1 $mA.cm^{-2}$	50 W LED lamp	-	Eslamluet. al 2023
4.	Pt-CdS/Cu_3BiS_3	photocathode	Chemical bath deposition (CBD)	~2 $mA.cm^{-2}$ (at 0 VRHE) and ~0.75 VRHE	AM 1.5G light irradiation	Na_2HPO_4/ NaH_2PO_4	Huang et al.2021
5.	TiO_2/CdS/ Cu_3BiS_3	Photocathode	Atomic layer deposition (ALD)	7 $mA.cm^{-2}$, ABPE of 1.7% at 0.4 VRHE, IPCE value increased from 15 to 44% at 450 nm	AM 1.5G light irradiation	Na_2HPO_4/ NaH_2PO_4	Huang et al.2021
6.	Cu_3BiS_3/TiO_2/ZnO		Sol-gel method	2.34 $mA.cm^{-2}$ at 1 V	Xe arc lamp (150W)	NaOH/ Na_2SO_4	Dutta et al.2021
7.	Pt-In_2S_3/ Cu_3BiS_3	photocathode	Sputtering	-110 µA cm^{-2} at 0 V	AM 1.5G simulated solar light	Na_2SO_4	Kamimura et al. 2017
8.	Cu_3BiS_3/TiO2	photocathode	Dip coating method	Photocurrent desity -1.4× 10−4 $A.cm^{-2}$ at -0.5 V vs Ag/AgCl low Tafel slope of 42.67 mV dec^{-1} a large current density of 10.8 $mA.cm^{-2}$ at the overpotential of 220 mV	300 W Xe lamp	Na_2SO_4	Li et al. 2018
9.	Au/ Cu_3BiS_3		solvothermal method	Photocurrent density of 2×10^{-4} $A.cm^{-2}$ at -0.5 V versus Ag/AgCl HER of 2.31 µmol h^{-1}	300 W Xe lamp	Na_2SO_4	Li et al. 2020

10.	Bi_2S_3–Cu_3BiS_3-$BiVO_4$ tandem	Photocathode – photoanode	CBD - sol gel method	STH efficiency of 2.33% photocurrent density of 7.8 $mA.cm^{-2}$ at 0 V	AM 1.5 G simulated solar light	0.5M K-Pi	Moon et al.2023
11.	Cu_3BiS_3/rGO/g-C_3N_4	Electrode	Sol gel method	overpotential of 111 and 205 mV to attain 10 $mA.cm^{-2}$ and 50 $mA.cm^{-2}$ current density (**electrocatalytic**) superior catalyst in alkaline solution	-	KOH	Swathi et al. 2023
12.	Cu_3BiS_3	Photocathode	Microwave irradiation	current density of 10 $mA.cm^{-2}$ Tafel slope was 251.07 mV/ dec charge transfer resistance (Rct) was 7.2 Ω	visible light (500 $mW.cm^{-2}$) irradiation	0.5 M Na_2SO_4	Wang et. al 2022
13.	Pt-TiO_2/$In_{0.6}Cd_{0.4}S$/Cu_3BiS_3	Photocathode	Spray pyrolysis method	photocurrent density of ≈12.20 $mA.cm^{-2}$ at 0 VRHE ABPE 3.13% STH of 2.57% for over 100 h HER found was 92 μmol h^{-1} in a buffer solution with pH 6.5	AM 1.5 G simulated solar light irradiation	0.2 mol L−1 Na_2HPO_4/NaH_2PO_4	Wu et al. 2022
14.	Cu_3BiS_3/TiO_2	Photocathode	Solvothermal method	Photocurrent density- 4.449 mA cm^{-2} fill factor (FF) is 60.8% conversion efficiency η (%) 1.281	CELL-S500 (China) solar simulator		Yin et al. 2014
15.	La_2CuO_4-GCEs	Electrode	wet-chemical method	band gap of 1.9 eV decrease in charge transfer resistance (223 kΩ) highest current of 250μA observed at pH 7	I_2–KI solution	0.1M phosphate buffer	Asiri et al. 2020
16.	La_2CuO_4:2%Ca	photocathode	doctor blade technique	Porosity found was 80 nm maximum efficiency of	50 W halogen	-	Spijkeret et al. 2008

				0.73% at 45 W/m^2 IPCE of 2% at 400 nm Only stable in alkaline solutions			
17.	Cu_2O/La_2CuO_4	Photocatalyst	polyethylene glycol gel method	Cu_2O greatly promotes efficient charge separation. H_2 production for 5% loaded Cu_2O photocatalyst found to be approx.~130 µmol	200-W Mercury–Xenon lamp	10% methanol/water solution	Zhang et al. 2013
18.	$LaFeO_3$/g-C_3N_4	Photocatalysis	Two step simple calcination method	The photocatalytic hydrogen production rate of LFO/CNNS-0.25G composite is 2.78, 162.36 and 1.96 times than that of CNNS, LFO and binary LFO/CNNS composite, respectively, Enhanced charge separation efficiency	300 W Xe lamp	0.5 M Na_2SO_4	Tian et al. 2022
19.	$LaFeO_3$/CdS/carbon quantum dots	Photocatalysis	Hydrothermal synthesis	Hydrogen evolution =25302 $\mu mol\ h^{-1}\ g_{cat}^{-1}$ Promoted charge transfer	Sun light illumination	Lactic acid aqueous solution	Manchala et al. 2020
20.	$LaFeO_3$-RGO-NiO	Photocatalysis	Sol gel method	Hydrogen generation = 89.2 $\mu mol.\ h^{-1}.\ g^{-1}$	125 W Xe lamp	10 vol% Methanol	Vijaayragvan et al.2020

21.	$LaFeO_3$/g-C_3N_4	Photocathode	magnetron sputtering	Photo current onset potential = 0.6 V_{RHE} hydrogen production rate of 10.8 µmol·h^{-1}·cm^{-2} Improves charge carrier separation Less charge carrier recombination	AM 1.5 G simulated solar light irradiation	0.1M Na_2SO_4	Guigoz et al. 2020

Table 2 2-methyl imidazole-based metal organic framework results in photoelectrochemical studies

S.No.	Metal	Photocatalyst / electrocatalyst	Role of MOF	Combination	Mode of preparation	Electrolyte	Conclusion	Ref
1.	Zn (ZIF-8)	Photoanode	positive role in carrier transport and separation	$BiVO_4$/Zn-MOF	Sol - gel technique	0.5 M Na_2SO_4	3.1 times of that of bare BiVO4 charge separation efficiency increased to 50.46%	Bai et al. 2022
2.	Co	Electrocatalyst	Provides large surface area	CoNi-SP/NPC	Sol -gel technique	1 M KOH	50 mA cm^{-2} at only 1.8 V overpotential for H_2 evolution 105 mV at 10 mA cm^{-2} O_2 evolution 313 mV at 100 mA cm^{-2}	Chen et al. 2023
3.	Co	photoanode	Shows synergistic effect with	$Ni_xCo_{1-x}O$/$BiVO_4$	Hydrothermal method	0.5 M Na_2SO_4	3.2 mAcm^{-2} at 1.23 V Higher porosity, charge separation efficiency and charge injection efficiency	Huang et al. 2023
4.	Co	photoanode	Reduce surface	α-Fe_2O_3@Ag@	Drop Casting	0.1 M NaOH	1.04 mA.cm^{-2} at 1.23 eV	Ji et al. 2023

			charge transfer resistance improved electron-hole pair separation and charge transport induced	ZIF-67			vs RHE improved visible light absorption	
5.	Zn, Co	Electrocatalyst	Precursor	NiCo-LDH/NF	Solvothermal	1.0 M KOH	400 mA cm^{-2} at overpotential 398 mV for OER high stability at 50 mA cm^{-2} for over 50 h	Shi et al. 2023
6.	Co	Photocatalyst	enhance the carrier separation efficiency improve the photocatalytic performance	ZIF-67- MBI	Sol - gel technique	0.5 M Na_2SO_4	H_2 evolution rate 6.14 mmol $g^{-1}h^{-1}$ oxygen evolution rates 210 mmol $g^{-1}h^{-1}$	Wang et al. 2023
7.	Co	photoanode	co – catalyst	$BiVO_4$-MOF-N2	Electrodeposition - Dip coating	0.5 M Na_2SO_4	2.32 mA·cm^{-2} highest charge transfer efficiency(63.1 %) at 1.3 V, low charge transfer resistivity	Wang et al. 2023
8.	Co	photoanode	charge separation	Co-MOF/Ti-Fe_2O_3	Hydrothermal and impregnation method	1 M NaOH	H_2 evolution rate 22.1 mmol.cm^{-2} photocurrent density of 1.01 mA.cm^{-2}	Cai et al. 2023

							(1.23VRHE) faradaic efficiency (FE, %) 97 and 100 for H2 and O2 charge separation increases 96.13%	
9.	Co	Photocatalyst	co-catalyst	ZIF/W: BVO OZIF/WBVO	Hydrothermal method	0.5 M Na_2SO_4	photocurrent densities of 2.30 & 2.04 mA/cm^2 at 1.23 V_{RHE} Larger band gap observed for ZIF/W:BVO and OZIF/W:BVO around 2.56 eV reduce charge recombination act as co-catalyst	Chen et al. 2023
10.	Co	photoanode	reduce charge recombination induce defect site generation	WBVO/O67	Hydrothermal/Drop casting	0.5 M Na_2SO_4	Photocurrent density of 2.08 $mA.cm^{-2}$ at 1.23 V_{RHE} reduce charge recombination largest carrier density the smallest resistances	Cheng et al. 2022
11.	Zn	Photoanode	suppresses photogenerated carrier recombination	TiO_2/Ag/ZIF-8	Hydrothermal method	mixture of Na_2SO_3 and Na_2S	photocurrent density of 250.2 $\mu A.cm^{-2}$ IPCE value = 88.4% Carrier density =1.85 × 1022	Deng et al. 2022

							m^{-3} the SPR effect of Ag NPs extends the absorption range of visible light suppression in photogenerated carrier recombination elevation in photogenerated charge transfer band gap observed at 2.75eV	
12.	Zn	Photocatalyst	-	ZIF-8 /(C)-ZnO/Ag_3PO_4	facile solution method	0.5 M Na_2SO_4	catalysts show a rate constant 27.5-fold higher than pristine ZIF-8 and 5-fold higher than ZnO catalysts	Dharman et al. 2023
13.	**Co**	Photoanode	capturing photogenerated holes visibly improve the photo response performance	Co_3O_4/TiO_2	electrostatic adsorption	1 M NaOH	photocurrent density of 1.04 $mA.cm^{-2}$ (1.23 V vs RHE) ($\eta_{injection}$) reached 81.74% ($\eta_{separation}$) reached 38.85% Band gap was 2.97 eV Heterojunctions promote the charge	Ding et al. 2021

							transfer performance and promote electron/hole separation	
14.	Co	photoanode	charge separation	Co-MOF/Ti-Fe_2O_3	Hydrothermal and impregnation method	1 M NaOH	H_2 evolution rate 22.1 mmol.cm^{-2} photocurrent density of 1.01 mA.cm^{-2} (1.23VRHE) faradaic efficiency (FE, %) 97 and 100 for H2 and O2 charge separation increases 96.13%	Gao et al. 2023
15.	**Co**	photoanode	reduce the charge carrier recombination rate enhanced light harvesting capability	Fe_2O_3/MIL-88B@ZIF-67	hydrothermal method	1 M NaOH	photocurrent density of 2.52 mA·cm^{-2} at 1.23 V IPCE =30.85% at 330 nm reduce the charge carrier recombination rate extraordinary stability of photoanode	Reddy et al. 2020
16.	Co	photoanode		BiVO4/ Co(O)OH	electrodeposition-annealing	0.5 M NaBi	Photocurrent density of 4.2 mA.cm^{-2} ABPE value of 1.22 % reduces the onset	Sun et al. 2021

							potential of $BiVO_4$ Co(O)OH cocatalyst serves as a hole extraction engine	
17.	Co	photoanode		TiO_2 -Co_3O_4	wet chemical method	0.5 M Na_2SO_4	photocurrent density of 2.4 $mA{\cdot}cm^{-2}$ at 1.23 V IPCE value was 57% temperature variation studies electron–hole separation increases increase the absorption of visible light activity reduction in charge transfer resistance	Thu et al. 2023
18.	Co	photoanode	Co-catalyst	WBVO/ZIF67-20	Electrodeposition / hydrothermal	0.5 M Na_2SO_4	photocurrent density of 2.30 $mA.cm^{-2}$ at 1.23 V Max. ABPE of 1.43% @0.67 VRHE R_{ct} -177 ohm create efficient charge transfer paths increase light absorption reduce	Wu et al. 2022

							charge recombination	
19.	Co	photoanode	Co-catalyst	CoZnMOF/B-BVO	SILAR method	0.5 M Na_2SO_4	Photocurrent density of 4.27 $mA.cm^{-2}$ HER found to be 26.2 µmol/h at 1.23 VRHE ABPE efficiency of 0.94% η_{inj} - 88.2% (vs 51.3%) η_{sep} - 91% (vs 43.5%) MOF increase the surface electron density Improve the catalytic kinetics	Xie et al. 2022
20.	Co	photoanode	Co-catalyst	$Co_3O_4/BiVO_4$	Dip coating	0.5 M KH_2PO_4	photocurrent density of 2.35 $mA.cm^{-2}$ (1.23 V vs RHE) IPCE of 26% (360 nm) HER found to be 0.61 $mmol.cm^{-2}$ improve the light absorption increase the charge separation reduce the charge recombination	Xu et al. 2019

21.	Zn (ZIF-8)	photoanode	Co-catalyst	Ni/ZnO/TiO_2	electrostatic adsorption / vacuum thermal evaporation	0.5 M Na_2SO_4 / KOH	photocurrent density of 1.34 $mA.cm^{-2}$ at 1.23 V resistance to photo corrosion Ni show the SPR effect band gap widths 2.96 eV	Xu et al. 2023
22.	Co	Photoanode	Co-catalyst	ZIF-67–150 s/$BiVO_4$	Electrodeposition	3.5 wt% NaCl solution	photocurrent density ~99 $\mu A.\ cm^{-2}$ band gap 2.01 eV increased visible light absorption increased in the carrier transport rate	Yang et al. 2023
23.	Co	Photoanode	Lewis acid	TiO_2-ZnNi		0.5 M Na_2SO_4	photocurrent density of 1.00 mA/cm2 (1.23 V vs. RHE) flat band potential (Efb)= 0.165 V IPCE = 34.33% $\eta_{injection}$ = 94.51% at 1.17 V vs RHE, 65.39% at 1.03 V vs RHE positive shift in flat band potential increases the separation of	Yu et al. 2022

							charge carriers no significance change was observed in absorption	

The effectiveness of a semiconductor photoelectrode hinges on the specific requirements have been outlined under section 1.2.1. To identify materials that possess those crucial properties and can serve as ideal candidates for photoelectrochemical (PEC) water splitting, a thorough examination of the available options is required. While various materials have been explored in the quest for suitable candidates, none from the reviewed studies have emerged as ideal contenders. Therefore, I conducted a comprehensive literature review focusing on several material classes, including metal oxides, chalcogenides, carbon-based materials, and metal-organic frameworks attached as table 1 & 2.

These materials, while showing promise within certain limits, necessitate structural, chemical, and electronic property modifications to exhibit efficient performance.

3.1 Metal Oxides (MOs)

Metal oxides (MOs) are inorganic semiconductor materials composed of metals (main and transition group elements) bonded to oxygen atoms. They offer stability, ease of synthesis, cost-effectiveness, and adaptability for post-modifications. Metal oxides (MOs) encompass a wide range of binary and ternary oxides, including zinc oxide (ZnO), titanium dioxide (TiO_2), cuprous oxide (Cu_2O), lanthanum ferrite or lanthanum iron oxide ($LaFeO_3$), lanthanum cuprate (La_2CuO_4), and more. While Metal oxides (MOs) have been actively used in photoelectrochemical (PEC) water splitting, they exhibit limitations in their electronic, optical, and structural properties, necessitating further research to enhance their candidacy. Metal oxides (MO) semiconductors encompass various sub-categories, such as binary oxides, perovskites (ABO_3), spinels (AB_2O_4), delafossites (ABO_2), and perovskite-like oxides (A_2BO_4) among other ternary oxides.

The present study concentrates on identifying materials that can effectively absorb visible light, minimize charge recombination rates, and yield high photocurrent densities. The absorption properties of metal oxides span both the ultraviolet (UV) and visible regions, with materials having band gaps

above 3-3.5 eV absorbing ultraviolet (UV) light (constituting 3-5% of solar radiation) and those with band gaps below 3 eV absorbing visible light (making up 42-45% of solar radiation at the Earth's surface).Therefore, the focus lies on binary and ternary Metal oxides (MOs), perovskites (ABO_3) and perovskite-like oxides (A_2BO_4).

3.1.1 Perovskites

The term "perovskite" originated when Russian mineralogist Lev Perovski identified calcium titanate ($CaTiO_3$) as the first perovskite material (Pattanayak et al.,2022). Perovskites constitute a ternary class of materials with the general formula ABX_3. In this formula, "A" represents alkali metals (Li, Na), alkaline-earth metals (Ba, Sr), or rare-earth metals (La, Pr), "B" encompasses various transition metals (Ti, Fe, Co, Mn, Ta), and "X" can be either an oxide or halide (Wang et al.,2015; Tan et al.,2017; Pattanayak et al., 2022).

Perovskite-like metal oxides (ABO_3) exhibit exceptional sunlight absorption, high activity and durability, outstanding compositional and structural flexibility, and precise control over band gaps and band edges. Lanthanum iron oxide ($LaFeO_3$) is a promising candidate due to its stability, environmental friendliness, and the relative abundance of its component elements. However, the fast recombination rate of electron-hole pairs challenges its efficiency in photocatalytic activity. This study aims to mitigate this challenge by employing surface modification, foreign atom doping, and heterojunction formation to facilitate efficient photocatalysis in the visible light region (Koli et al.,2021; Yadav et al.,2023; Jayanthi et al.,2022; Samjhdar et al.,2023; Kumari et al.,2022).

3.1.2 Other Notable Perovskite-Like Oxides

Another notable perovskite-like oxide is Lanthanum cuprate (La_2CuO_4), characterized by its tetragonal K_2NiF_4-structured layered perovskite oxide form. This oxide structure, known as Ruddlesden-Popper oxide-based layered perovskites, has gained attention for its unique physical properties, including superconductivity, ferroelectricity, photoluminescence, photocatalytic activity, and electrocatalysis. It exhibits stoichiometric variations across different temperature ranges, displaying superconducting behavior at low temperatures and semiconductor characteristics at optimal stoichiometry. While various studies have explored its nanoparticle and crystallite forms for optical, electronic, and photoelectronic properties, challenges persist due to the unfavorable position of its valence band for oxygen evolution,

leading to photo corrosion. Addressing these challenges will be a central focus of this study, utilizing cost-effective modification strategies to enhance its suitability for photoelectrochemical (PEC) water splitting (Asiri et al.,2020; James et al.,2020; Parida et al.,2020; Singh et al.,2019; Longo et al.,1972; James et al.,2020; Wang et al.,2022).

3.2 Metal Organic Frameworks (MOFs)

The term "metal-organic frameworks (MOF)" was initially coined in 1995 by Professor Omar Yaghi and colleagues, even though research on metal-organic frameworks (MOFs) started in the late 1990s, and the first visible-light metal-organic frameworks (MOFs) composite photocatalyst was published in 2009 (Dutta et al.,2021). Metal-Organic Frameworks (MOFs), also known as porous coordination polymers (PCPs) (Xiao et al.,2020), represent a novel and burgeoning class of materials. They consist of infinite lattices formed from inorganic secondary building units (SBUs), which can be metal ions or clusters of alkaline earth metals, first-row transition metals, lanthanides, and organic linkers like imidazole and aromatic carboxylic acids. These building blocks are held together by moderately strong coordination bonds as shown in fig 2. (Zheng et al.,2018; Aretra et al.,2017; Sun et al.,2023)

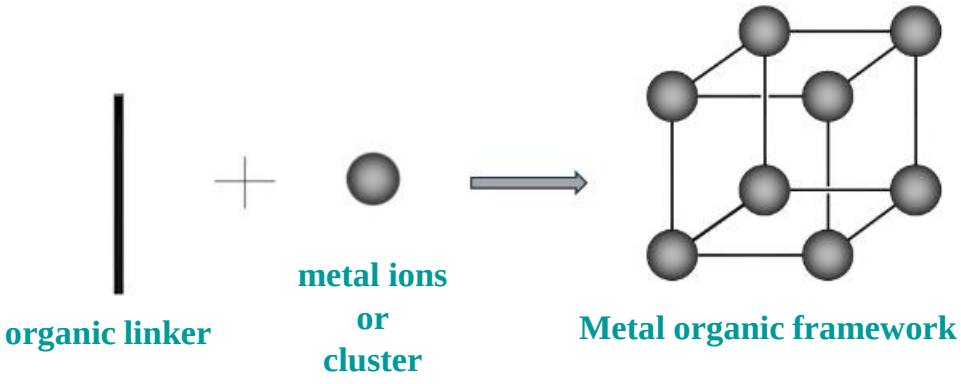

Figure 2 Structural Unit of Metal Organic Framework

Metal-Organic Frameworks (MOFs) boast distinctive qualities, including structural flexibility, a large specific surface area (up to 6000 m^2g^{-1}), high porosity (approximately 90%), controllable pore sizes (0.5-2 nm), ideal metal placement, unique electronic band structures, numerous active sites, cost-effective synthesis, and ease of modification. Consequently, they have garnered significant attention in the field of photoelectrochemical (PEC) research. In general, most metal-organic frameworks (MOFs) are insulators and serve as high surface area supports for semiconducting nanostructured catalytic centers

with precisely ordered atom arrangements. Some metal-organic frameworks (MOFs) are used as co-catalysts, templates alongside dyes, or composite semiconductors to enhance kinetic processes, reduce electron/hole recombination and increase light absorption. Modification strategies can easily alter the functional band gaps of metal-organic frameworks (MOFs) by introducing various functional groups to the linkers. The post-modification strategies rely on aspects like structural formation (nanostructures, core-shell, hollow structures, etc.) and the presence of linked ligands. These modifications effectively lower the band gap for visible light by introducing functional groups such as amino and porphyrin groups to organic linkers, extending the light-absorption capabilities.

Among various class of metal-organic frameworks (MOFs) based on the organic linker and transition metal viz, metal-organic frameworks (MOFs) classified as the zeolite imidazolate frameworks (ZIFs) produced from imidazole-based ligands and transition-metal cations (e.g., Co,Ni,Zn...) specifically zeolite imidazolate framework(ZIF-8) (composed of Zn as metal center with 2-methyl imidazole as linker) & zeolite imidazolate framework(ZIF-67) (composed of Co, Ni as metal center with 2-methyl imidazole as linker) will be used in the present study. These metal-organic frameworks (MOFs) owing to their high thermal and chemical stability, abundant active sites, large band gap have grabbed the attention of the researchers towards their applicability in photoelectrochemical (PEC) water splitting application. Therefore, the present study will be explored for the modification of working electrode (thin films) of metal oxide, Perovskites, Chalcogenides class of material through ZIF-8, ZIF-68 (Obeidli et al.2021; Xiao et al.,2020; Tao Wang et al.,2023; Dharman et al.,2023).

3.3 Carbon-Based Materials

Carbon-based materials have gained extensive attention in the fields of electrocatalysis and photocatalysis in recent years due to their low toxicity, abundance in nature, excellent electrical, optical, and magnetic properties, large surface area, tunable electronic structures, thermal and mechanical stability. Various carbon-based nanomaterials, including graphene, carbon nanotubes (CNTs), multi-walled carbon nanotubes (MWCNTs), graphitic carbon nitride (g-C_3N_4), carbon quantum dots (QDs), and fullerenes, have been studied. Among these, graphene has been a focus of significant interest due to its two-dimensional hexagonal honeycomb-like π-conjugated structure, which provides exceptional properties such as a large surface area (2600-2630 m^2 g^{-1}), high optical transparency (90-97.7%),

ultrafast electron transfer (200,000 $cm^2V^{-1}s^{-1}$), high thermal conductivity ($5000Wm^{-1}K^{-1}$), and a long mean free path (Srivastava et al.,2023; Diaz et al.,2023; Ahmed et al.,2019).

Besides graphene, carbon nanotubes (CNTs) also gained a lot of interest in the application of water splitting. Carbon nanotubes (CNTs) possess the greater specific surface area, which boosts the activity to capture electrons from the metal center, prevent charge recombination, and promote the interfacial electron transfer process. Because of exceptionally high electronic as well as catalytic properties, it behaves synergically with the semiconductor material. As per the reported literature, carbon nanotubes (CNTs) solely as a photoelectrode do not offer a photoelectrochemical (PEC) response given that they agglomerate immediately due to strong Vander Waals interactions, limiting their own conductive effect and providing a more resistant channel for charge carrier transit. Therefore, the present study will be focused to analyse its effect as a modifying material for working of prepared electrode (Zhang et al.,2021; Ali et al.,2021, Sankhula et al.,2023; Rai et al.,2016; Lei at al.,2021).

3.4 Chalcogenides

Chalcogenides are compounds consisting of a ternary metal associated with a chalcogen element, such as copper tin selenide(Cu_2SnSe_3), copper bismuth sulfide (Cu_3BiS_3), copper antimony sulfide (Cu_3SbS_4), and more. During the literature survey, we found that this class of materials exhibits the essential characteristics needed for efficient solar energy absorption. This includes a low band gap energy, high photo-absorption ability, and a crystalline nature. Chalcogenide compounds have been extensively studied in the fields of solar cells and photovoltaics. Among these materials, Cu-based chalcogenides have gained considerable interest due to their ideal properties for efficient photoelectrode operation in photoelectrochemical (PEC) water splitting.

Copper bismuth sulfide (Cu_3BiS_3), a ternary compound belonging to the I-V-VI family, occurs naturally as the Wittichenite mineral. It is composed of abundant and low-cost elements, displays low toxicity, has a direct band gap energy of 1.40 - 1.86 eV, a high optical absorption coefficient in the visible region ($\alpha > 10^4\ cm^{-1}$), and exhibits p-type semiconductor behavior with an orthorhombic crystal structure. In view of these distinctive features, as well as the limitations of photo-corrosion challenges, further investigation into the application of photoelectrochemical (PEC) water splitting is required.

In conclusion, we have planned to prepare thin films based photoelectrochemical (PEC) electrode of

$LaFeO_3$, La_2CuO_4 and Cu_3BiS_3. MOF (ZIF-8, ZIF-67), carbon nanotubes (CNTs) will be explored for the modification of the prepared electrode. Table 3. Shown the summary of chosen material for the electrode preparation.

Table 3 Summary of material of interest

Material	Bandgap (eV)	Valence Band (VB)	Conduction Band (CB)	Properties
$LaFeO_3$	2.1 – 2.6	2.5	-0.27	Perovskite (ABO_3) P-type semiconductor material Narrow Band gap Visible light active Photocathode **Limitation** Fast charge recombination
La_2CuO_4	1.2 - 3.6	0.4	-1.36	Perovskite like oxide (A_2BO_4) P-type semiconductor material Narrow Band gap Visible light active Photocathode Stable in alkaline medium **Limitation** Valence band position
Cu_3BiS_3	1.40 -1.86	0.78	-0.52	Chalcogenides P-type semiconductor material Narrow Band gap High optical absorption coefficient Visible light active Photocathode Free carrier concentration ($2\times 1016\ cm^{-3}$) **Limitation** Photo-corrosion Valence band position

4. Proposed Work

4.1 Proposed Study

The motivation for the proposed work stems from the need to design effective photoelectrochemical (PEC) systems for solar hydrogen generation. The primary focus of the study will be on the fabrication and characterization of specific layered and doped materials and how effectively they function in water photo-splitting. Chemically stable materials based on perovskites, graphene, metal-organic frameworks, and chalcogenides, primarily absorbing the visible range, will be of interest. The principal goal is to investigate to what extent semiconductor nanostructures and nanoarchitectures enhance the photoelectrochemical (PEC) response for water splitting. The study will address a series of objectives

and stages.

4.2 Objectives/Stages of the Proposed Work

The study will primarily focus on photoelectrochemical investigations of the materials of interest for photoelectrochemical water splitting. The objectives and stages of the proposed work will include:

a) Preparation of nano heterostructure/ heterojunction based thin films using wet chemical methods (such as sol-gel or spray pyrolysis)

b) Characterization of samples based on parameters outlined in Table 4.

c) Conducting photoelectrochemical (PEC) investigations related to the photo-splitting of water using samples prepared under objective "a".

Table 4 Tentative plan of the proposed work

Parameters of the study	**Description**
Preparation of samples ● Materials of interest	Few of the following: ZnO, La_2CuO_4, TiO_2, $LaFeO_3$, Cu_3BiS_3, Modification: MOF (ZIF-8, ZiF-67), CNTs
Proposed Avenues for Investigation	Nanostructures/Nanoarchitectures Layered structures / Heterojunctions Core Shell structures
Proposed method for the preparation of samples	Wet chemical process (Sol-gel or spray pyrolysis), Hydrothermal
Expected variables in the study	***Preparation of samples:*** Nature of metal oxides and their combinations Sintering Conditions: Temperature, Environment, photoelectrochemical (PEC) studies: pH variation, electrolyte variation
Characterization	Phase analysis by X-ray Diffraction (XRD) Surface morphology by Field Emission Scanning Electron Microscope (FE- SEM) Elemental composition and stoichiometry by EDX and XPS analyses Surface Topography by Atomic Force Microscope (AFM) Charge carrier dynamics by Electrochemical Impedance Spectroscopy (Nyquist Plot) Band gap energy by UltraViolet (UV)-Vis spectrophotometer Flat band potential and charge carrier density by Mott-Schottky
PEC measurement variables	Current-Voltage characteristics of the photoelectrochemical(PEC) cell under darkness and illumination. Photovoltage & Photocurrent Open circuit potential Short Circuit current Onset voltage

	Applied bias photon to current conversion efficiency (ABPE) Chronoamperometry (stability of semiconductor material)

4.3 Proposed Methodology

In the proposed methodology, thin films will be fabricated through wet chemical routes utilizing precursor solutions. These films will be deposited onto conducting glass substrates through techniques like spin-coating or spray pyrolysis. Subsequently, the samples will undergo a high-temperature sintering process to promote crystalline phase development. Comprehensive characterization of all prepared samples will be carried out using standard methods, encompassing structural analysis, morphological examinations, electrical/electronic assessments, and optical property evaluations. Characterization tools will include X-ray diffractometers, scanning electron microscopes, atomic force microscopes, and Ultra Violet (UV)-visible spectrometers. For photoelectrochemical (PEC) studies, the prepared samples will be employed as working electrodes (WE) within photoelectrochemical (PEC) cells, and xenon arc light sources will provide illumination.

4.4 Modification Strategies

Building upon the previous discussion, the semiconductor photoelectrode will be tailored to maximize visible light activity while enhancing stability through various modification techniques. These strategies include surface modifications, structural adjustments facilitated by heterojunction formation, doping strategies, and the incorporation of co-catalysts and photosensitizers. By implementing these techniques, the study aims to maximize light absorption while mitigating impediments to other essential functions in the semiconductor photoactive material.

5. Expected Outcome

The anticipated outcomes of this research encompass an augmented photocurrent density, reduced overpotential relative to pristine materials, and enhanced stability of semiconductor materials. These outcomes hold the potential to provide a environmentally friendly solution for efficient green and solar hydrogen generation.

6. Conclusion

In conclusion, this work plan outlines a comprehensive approach to studying and improving

photoelectrochemical systems for water splitting, with a focus on green hydrogen production. The plan encompasses various stages, objectives, and methodologies designed to address the challenges associated with harnessing solar energy for sustainable hydrogen generation.

The proposed work aims to develop and characterize thin films through wet chemical routes, laying the foundation for the investigation of their structural, morphological, electrical, and optical properties. These materials will serve as working electrodes in photoelectrochemical cells, where their performance will be evaluated under xenon arc light illumination.

Modification strategies, including surface modifications, structural enhancements through heterojunction formation, doping strategies, and the incorporation of co-catalysts and photosensitizers, will be employed to maximize visible light absorption and improve the stability of semiconductor materials.

The expected outcomes include an increase in photocurrent density, a reduction in overpotential, and enhanced stability of semiconductor materials. These improvements will contribute to the development of a environmentally friendly method for efficient green and solar energy driven hydrogen production. In summary, this work plan sets the stage for research that addresses critical global challenges related to energy, sustainability, and environmental conservation. The potential for generating green hydrogen through advanced photoelectrochemical systems offers a promising solution to these challenges and paves the way for a more sustainable and greener future.

REFERENCES

Aghakhani, A., Haque, N., Saccani, C., Pellegrini, M., & Guzzini, A. (2023). Direct carbon footprint of hydrogen generation via PEM and alkaline electrolysers using various electrical energy sources and considering cell characteristics. *International Journal of Hydrogen Energy*, *48*(77), 30170-30190.

Ahmed, A. M., Mohamed, F., Ashraf, A. M., Shaban, M., Khan, A. A. P., & Asiri, A. M. (2020). Enhanced photoelectrochemical water splitting activity of carbon nanotubes@ TiO_2 nanoribbons in different electrolytes. *Chemosphere*, *238*, 124554.

Al Obeidli, A., Salah, H. B., Al Murisi, M., & Sabouni, R. (2022). Recent advancements in MOFs synthesis and their green applications. *International Journal of Hydrogen Energy*, *47*(4), 2561-

2593.

Ali, M., Pervaiz, E., Sikandar, U., & Khan, Y. (2021). A review on the recent developments in zirconium and carbon-based catalysts for photoelectrochemical water-splitting. *International Journal of Hydrogen Energy*, *46*(35), 18257-18283.

Asiri, A. M., Adeosun, W. A., & Rahman, M. M. (2020). Development of highly efficient non-enzymatic nitrite sensor using La2CuO4 nanoparticles. *Microchemical Journal*, *159*, 105527.

Bai, H., Wang, F., You, Z., Sun, D., Cui, J., & Fan, W. (2022). Fabrication of Zn-MOF decorated $BiVO_4$ photoanode for water splitting. *Colloids and Surfaces A: Physicochemical and Engineering Aspects*, *640*, 128412.

Cai, J., Tang, X., Zhong, S., Li, Y., Wang, Y., Liao, Z., ... & Xie, Q. (2023). Elucidation the role of Co-MOF on hematite for boosting the photoelectrochemical performance toward water oxidation. *International Journal of Hydrogen Energy*, *48*(33), 12342-12353.

Chen, C., Pai, H., Chen, H., Yougbaré, S., Husain, S., Hsiao, Y., & Lin, L. (2023). Distinguished heterojunction and co-catalyst behaviors on tungsten doped $BiVO_4$ for photoelectrochemical catalytic water splitting reaction. *Materials Today Sustainability*, *24*, 100488.

Chen, S., Liang, W., Wang, X., Zhao, Y., Wang, S., Li, Z., ... & Gao, F. (2023). P-doped MOF-derived CoNi bimetallic sulfide electrocatalyst for highly-efficiency overall water splitting. *Journal of Alloys and Compounds*, *931*, 167575.

Chen, Y., Zheng, W., Murcia-Lopez, S., Lv, F., Morante, J. R., Vayssieres, L., & Burda, C. (2021). Light management in photoelectrochemical water splitting–from materials to device engineering. *Journal of Materials Chemistry C*, *9*(11), 3726-3748.

Cheng, T. M., Pai, H., Hsu, C. S., Kubendhiran, S., Yougbaré, S., Lin, L. Y., & Wu, Y. F. (2023). Incorporation of oxidized zeolitic imidazolate framework 67 as effective Co-catalyst on W-doped $BiVO_4$ for catalyzing photoelectrochemical water oxidation. *International Journal of Hydrogen Energy*, *48*(13), 5152-5165.

Deng, J., Gao, J., Liu, M., Zheng, L., Wang, Y., Wang, Y., ... & Liu, Y. (2023). Construction of Z-scheme TiO_2/Ag/ZIF-8 nanorod array film with boosting photocatalytic and photoelectrochemical properties. *Journal of Alloys and Compounds*, *932*, 167680.

Dharman, R. K., Mariappan, A., & Oh, T. H. (2023). Accelerated photocatalytic degradation of sulfonamide antibiotic pollutant using oxygen vacancy in metal-organic framework ZIF-8/Ag_3PO_4 heterostructure. *Surfaces and Interfaces*, *39*, 102998.

Ding, Q., Gou, L., Wei, D., Xu, D., Fan, W., & Shi, W. (2021). Metal-organic framework derived Co_3O_4/TiO_2 heterostructure nanoarrays for promote photoelectrochemical water splitting. *International Journal of Hydrogen Energy*, *46*(49), 24965-24976.

Dong, G., Yan, L., & Bi, Y. (2023). Advanced oxygen evolution reaction catalysts for solar-driven photoelectrochemical water splitting. *Journal of Materials Chemistry A*, *11*(8), 3888-3903.

Dutta, R., Goyal, V., Srivastava, M., & Shrivastav, R. (2021). Double heterojunction system of $TiO_2/ZnO/Cu_3BiS_3$ for photoelectrochemical water splitting. *SPAST Abstracts*, *1*(01).

Dutta, R., Shrivastav, R., Srivastava, M., Verma, A., Saxena, S., Biswas, N. K., ... & Dass, S. (2022). MOFs in photoelectrochemical water splitting: New horizons and challenges. *International Journal of Hydrogen Energy*, *47*(8), 5192-5210.

Gao, M., Nguyen, N. T., Gao, R. T., Liu, X., Zhang, X., & Wang, L. (2023). Engineering single Pt Atoms on hybrid amorphous/crystalline CoFe layered double hydroxide accelerates the charge transfer for solar water splitting. *Applied Catalysis B: Environmental*, *336*, 122920.

Guigoz, V., Balan, L., Aboulaich, A., Schneider, R., & Gries, T. (2020). Heterostructured thin $LaFeO_3$/g-C_3N_4 films for efficient photoelectrochemical hydrogen evolution. *International Journal of Hydrogen Energy*, *45*(35), 17468-17479.

Guo, Z., & Liu, Z. (2021). Synthesis and control strategies of nanomaterials for photoelectrochemical water splitting. *Dalton Transactions*, *50*(6), 1983-1989.

Hemmati-Eslamlu, P., Habibi-Yangjeh, A., Akinay, Y., & Cetin, T. (2023). Novel g-C_3N_4 nanorods/Cu_3BiS_3 nanocomposites: Outstanding photocatalysts with pn heterojunction for impressively detoxification of water under visible light. *Journal of Photochemistry and Photobiology A: Chemistry*, *443*, 114862.

Huang, D., Li, L., Wang, K., Li, Y., Feng, K., & Jiang, F. (2021). Wittichenite semiconductor of Cu_3BiS_3 films for efficient hydrogen evolution from solar driven photoelectrochemical water splitting. *Nature communications*, *12*(1), 3795.

Huang, J., Luo, W., Yuan, X., & Wang, J. (2023). Bimetallic MOF-derived oxides modified $BiVO_4$ for enhanced photoelectrochemical water oxidation performance. *Journal of Alloys and Compounds*, *930*, 167397.

James, R. (2020). *Electrical properties of La_2CuO_4 and Nd_2CuO_4 and their coexistent pn heterojunction* (Master's thesis).

Jayanthi, G., Sumathi, S., Kannan, K., Andal, V., & Murugan, S. (2022). A Review on Synthesis, Properties, and Environmental Application of Fe-Based Perovskite. *Advances in Materials Science and Engineering*, *2022*(1), 6607683.

Ji, C., Xu, J., Jiang, Q., Kerherve, G., Zhou, H., Li, X., ... & Xie, F. (2023). Significantly boosted photoelectrochemical water splitting performance by plasmonic enhanced Hematite@MOF composite photoelectrodes. *Materials Today Advances*, *18*, 100361.

Kamimura, S., Beppu, N., Sasaki, Y., Tsubota, T., & Ohno, T. (2017). Platinum and indium sulfide-modified Cu_3BiS_3 photocathode for photoelectrochemical hydrogen evolution. *Journal of Materials Chemistry A*, *5*(21), 10450-10456.

Koli, P. B., Kapadnis, K. H., Deshpande, U. G., Tupe, U. J., Shinde, S. G., & Ingale, R. S. (2021). Fabrication of thin film sensors by spin coating using sol-gel $LaCrO_3$ Perovskite material modified with transition metals for sensing environmental pollutants, greenhouse gases and relative humidity. *Environmental Challenges*, *3*, 100043.

Koyale, P. A., & Delekar, S. D. (2024). A review on practical aspects of CeO_2 and its composites for photoelectrochemical water splitting. *international journal of hydrogen energy*, *51*, 515-530.

Kulshreshtha, Amit. "Clean Energy Transition Road Map for India." *Available at SSRN 4324235* (2023).

Kumari, M., Dhariwal, N., Kumar, V., & Thakur, O. P. (2023). Synthesis of p-$LaFeO_3$–n-$BaTiO_3$ heterojunctions and their room temperature methanol sensing applications. *IEEE Sensors Journal*, *23*(10), 10301-10307.

Kurnia, F., Scott, J. A., Valanoor, N., & Hart, J. N. (2023). A review of non-oxide semiconductors for photoelectrochemical water splitting. *Journal of Materials Chemistry C*, *11*(3), 802-826.

Lei, Y., Ossonon, B. D., Chen, J., Perreault, J., & Tavares, A. C. (2021). Electrochemical

characterization of graphene-type materials obtained by electrochemical exfoliation of graphite. *Journal of Electroanalytical Chemistry*, *887*, 115084.

Li, J., Zhao, Y., Han, X., & Xiao, D. (2021). A facile strategy for fabricating particle-on-flower Au-Cu_3BiS_3 nanostructures for enhanced photoelectrocatalytic activity in water splitting. *New Journal of Chemistry*, *45*(3), 1231-1239.

Li, J., Han, X., Wang, M., Zhao, Y., & Dong, C. (2018). Fabrication and enhanced hydrogen evolution reaction performance of a Cu_3BiS_3 nanorods/TiO_2 heterojunction film. *New Journal of Chemistry*, *42*(6), 4114-4120.

Longo, J. M., & Raccah, P. M. (1973). The structure of La_2CuO_4 and $LaSrVO_4$. *Journal of Solid State Chemistry*, *6*(4), 526-531.

Luo, J., Yang, H., Liu, Z., Li, F., Liu, S., Ma, J., & Liu, B. (2019). Organic-inorganic hybrid perovskite–TiO_2 nanorod arrays for efficient and stable photoelectrochemical hydrogen evolution from HI splitting. *Materials Today Chemistry*, *12*, 1-6.

Manchala, S., Gandamalla, A., Vempuluru, N. R., Venkatakrishnan, S. M., & Shanker, V. (2021). High potential and robust ternary $LaFeO_3$/CdS/carbon quantum dots nanocomposite for photocatalytic H_2 evolution under sunlight illumination. *Journal of Colloid and Interface Science*, *583*, 255-266.

Efficiency, S. (2023). Mixed Phase Interlayer for High-Performance Cu. *Adv. Sci*, *10*, 2206286.

Oar-Arteta, L., Wezendonk, T., Sun, X., Kapteijn, F., & Gascon, J. (2017). Metal organic frameworks as precursors for the manufacture of advanced catalytic materials. *Materials Chemistry Frontiers*, *1*(9), 1709-1745.

Parida, S., Brahma, S. S., Nanda, J., Sethy, S. K., & Sankaran, K. J. (2023). Spin coated La_2CuO_4 thin film: An extensive study on optical dispersion parameters. *Optik*, *278*, 170728.

Pattanayak, P., Singh, P., Bansal, N. K., Paul, M., Dixit, H., Porwal, S., ... & Singh, T. (2022). Recent progress in perovskite transition metal oxide-based photocatalyst and photoelectrode materials for solar-driven water splitting. *Journal of Environmental Chemical Engineering*, *10*(5), 108429.

Peón-Díaz, Francisco J., et al. "The effect of oxidative functionalization of carbon nanotubes on the

morphological, optical, and photoelectrochemical properties of modified titanium dioxide photoanodes." *Journal of Materials Science* 58.12 (2023): 5372-5388.

Rai, S., Ikram, A., Sahai, S., Dass, S., Shrivastav, R., & Satsangi, V. R. (2017). CNT based photoelectrodes for PEC generation of hydrogen: a review. *International Journal of Hydrogen Energy*, *42*(7), 3994-4006.

Reddy, D. A., Reddy, K. A. J., Gopannagari, M., Kumar, D. P., & Kim, T. K. (2020). Synergetic catalytic behavior of dual metal-organic framework coated hematite photoanode for photoelectrochemical water splitting performance. *Journal of Catalysis*, *391*, 471-479.

Samajdar, S., Bera, S., Das, P. S., Finch, H., Dhanak, V. R., Chakraborty, S., ... & Ghosh, S. (2023). Exploration of 1D-2D $LaFeO_3$/RGO S-scheme heterojunction for photocatalytic water splitting. *International Journal of Hydrogen Energy*, *48*(47), 17838-17851.

Sankhula, L., Lavate, S., & Srivastava, R. (2023). Advanced carbon-based nanomaterials for photoelectrochemical water splitting. In *Solar-driven green hydrogen generation and storage* (pp. 103-128). Elsevier.

Saraswat, S. K., Rodene, D. D., & Gupta, R. B. (2018). Recent advancements in semiconductor materials for photoelectrochemical water splitting for hydrogen production using visible light. *Renewable and Sustainable Energy Reviews*, *89*, 228-248.

Shi, X., Li, J., Zhang, X., & Guo, J. (2023). MOF derived NiCo-LDH hollow structure for oxygen evolution reaction. *Journal of Physics and Chemistry of Solids*, *172*, 111051.

Singh, R. P., Arora, P., Nellaiappan, S., Shivakumara, C., Irusta, S., Paliwal, M., & Sharma, S. (2019). Electrochemical insights into layered La_2CuO_4 perovskite: Active ionic copper for selective CO_2 electroreduction at low overpotential. *Electrochimica Acta*, *326*, 134952.

Sun, H., Hua, W., Liang, S., Li, Y., & Wang, J. G. (2022). Boosting photoelectrochemical activity of bismuth vanadate by implanting oxygen-vacancy-rich cobalt (oxy) hydroxide. *Journal of Colloid and Interface Science*, *611*, 278-286.

Sun, K., Qian, Y., & Jiang, H. L. (2023). Metal-organic frameworks for photocatalytic water splitting and CO_2 reduction. *Angewandte Chemie*, *135*(15), e202217565.

Swathi, S., Yuvakkumar, R., Ravi, G., Arunmetha, S., Arun, A., & Velauthapillai, D. (2024). Bayberry-

like Cu_3BiS_3 with 2D layered nanosheets of rGO and g-C_3N_4 for effective electrochemical HER activity. *International Journal of Hydrogen Energy*, *49*, 295-308.

Tan, P., Liu, M., Shao, Z., & Ni, M. (2017). Recent advances in perovskite oxides as electrode materials for nonaqueous lithium–oxygen batteries. *Advanced Energy Materials*, *7*(13), 1602674.

Tao, R., Sun, Z., Li, F., Fang, W., & Xu, L. (2019). Achieving organic metal halide perovskite into a conventional photoelectrode: outstanding stability in aqueous solution and high-efficient photoelectrochemical water splitting. *ACS Applied Energy Materials*, *2*(3), 1969-1976.

Tayebi, M., & Lee, B. K. (2019). Recent advances in $BiVO_4$ semiconductor materials for hydrogen production using photoelectrochemical water splitting. *Renewable and sustainable energy reviews*, *111*, 332-343.

Thanh Thu, C. T., Jo, H. J., Koyyada, G., Kim, D. H., & Kim, J. H. (2023). Enhanced Photoelectrochemical Water Oxidation Using TiO_2-Co_3O_4 p–n Heterostructures Derived from in Situ-Loaded ZIF-67. *Materials*, *16*(15), 5461.

Tian, Z., Yang, X., Chen, Y., Wang, X., Jiao, T., Zhao, W., ... & Hu, J. (2022). Construction of $LaFeO_3$/g-C_3N_4 nanosheet-graphene heterojunction with built-in electric field for efficient visible-light photocatalytic hydrogen production. *Journal of Alloys and Compounds*, *890*, 161850.

Van't Spijker, H., Simon, D., & Ooms, F. (2008). Photocatalytic water splitting by means of undoped and doped La_2CuO_4 photocathodes. *International Journal of Hydrogen Energy*, *33*(22), 6414-6419.

Vijayaraghavan, T., Althaf, R., Babu, P., Parida, K. M., Vadivel, S., & Ashok, A. M. (2021). Visible light active $LaFeO_3$ nano perovskite-RGO-NiO composite for efficient H_2 evolution by photocatalytic water splitting and textile dye degradation. *Journal of Environmental Chemical Engineering*, *9*(1), 104675.

Wang, Dan, et al. "Promoting photoelectrochemical water oxidation of $BiVO_4$ photoanode via Co-MOF-derived heterostructural cocatalyst." *Applied Surface Science* 619 (2023): 156710.

Wang, T., Guo, C., Zhang, L., Zhang, L., Cao, X., Akram, N., ... & Wang, J. (2023). Comparison of modulation strategies for enhancing the photocatalytic water splitting performance of metal-

organic frameworks. *Journal of Physics and Chemistry of Solids*, *175*, 111223.

Wang, W., Xu, M., Xu, X., Zhou, W., & Shao, Z. (2020). Perovskite oxide based electrodes for high-performance photoelectrochemical water splitting. *Angewandte Chemie International Edition*, *59*(1), 136-152.

Wang, W., Zhi, G., Liu, L., Fei, Y., Sheng, Q., Shi, Y., ... & Qian, H. (2022). Rapid Microwave Irradiation Synthesis and Photoelectrochemical Performance of Cu_3BiS_3 Nanoparticles. *Electronic Materials Letters*, *18*(6), 578-582.

Wang, W., Tadé, M. O., & Shao, Z. (2015). Research progress of perovskite materials in photocatalysis-and photovoltaics-related energy conversion and environmental treatment. *Chemical Society Reviews*, *44*(15), 5371-5408.

Wang, X. T., Li, B., Kong, D. R., Zhang, Z. Y., Zhang, X. F., Deng, Z. P., ... & Gao, S. (2022). T-and T′-type layered perovskite Ln_2CuO_4 nanocrystals for enhanced sensing detection of hydrogen peroxide. *Journal of Alloys and Compounds*, *911*, 165037.

Wu, X., Zhao, W., Hu, Y., Xiao, G., Ni, H., Ikeda, S., ... & Jiang, F. (2022). Research on the influence of the interfacial properties between a Cu_3BiS_3 film and an $In_xCd_{1-x}S$ buffer layer for photoelectrochemical water splitting. *Advanced Science*, *9*(33), 2204029.

Wu, Y. F., Pai, H., Kubendhiran, S., Yougbaré, S., & Lin, L. Y. (2022). Size effects of zeolitic imidazolate framework 67 polyhedrons as Co-catalyst of W-doped $BiVO_4$ electrodes for photoelectrochemically catalytic water oxidation. *International Journal of Hydrogen Energy*, *47*(97), 40961-40971.

Xiao, X., Zou, L., Pang, H., & Xu, Q. (2020). Synthesis of micro/nanoscaled metal–organic frameworks and their direct electrochemical applications. *Chemical Society Reviews*, *49*(1), 301-331.

Xie, J., Wang, L., Ren, J., Lu, X., Zou, L., Wang, S., & Yang, P. (2022). Oxidation state modulation of CoMOF with Zn for accelerating photoelectrochemical water oxidation of borate-irradiation treated $BiVO_4$. *Electrochimica Acta*, *421*, 140483.

Xu, J., Li, Z., Liu, Z., Xu, S., & Liu, X. (2023). Zn-MOF loading Cu_2O cube to construct hierarchical solid cage to improve photocatalytic hydrogen evolution. *Journal of Industrial and Engineering Chemistry*, *126*, 557-567.

Yadav, R., Modi, A., Dubey, K., & Malik, M. M. (2023). Optical and photoluminescence response driven by sintering temperature in $LaFeO_3$ nano-perovskites. *Journal of Materials Science: Materials in Electronics*, *34*(15), 1243.

Yang, Z., Li, H., Zhu, J., Li, W., Li, Y., & Zhang, P. (2023). Preparation of ZIF-67/$BiVO_4$ composite photoanode and its enhanced photocathodic protection performance of 316 SS under visible light. *Journal of Alloys and Compounds*, *961*, 170926.

Yin, J., & Jia, J. (2014). Synthesis of Cu_3BiS_3 nanosheet films on TiO_2 nanorod arrays by a solvothermal route and their photoelectrochemical characteristics. *CrystEngComm*, *16*(13), 2795-2801.

Yu, L., Ding, Q., Liu, Y., Sun, D., Ding, J., Zhu, G., ... & Fan, W. (2022). An in-situ cation exchange approach to stabilize Zn-MOF: Understanding the role of nickel ions for photoelectrochemical performance. *International Journal of Hydrogen Energy*, *47*(18), 10277-10288.

Zhang, Z., Chen, X., Zhang, X., Lin, H., Lin, H., Zhou, Y., & Wang, X. (2013). Synthesis of Cu_2O/La_2CuO_4 nanocomposite as an effective heterostructure photocatalyst for H_2 production. *Catalysis Communications*, *36*, 20-24.

Zheng, Y., Zheng, S., Xue, H., & Pang, H. (2018). Metal-organic frameworks/graphene-based materials: preparations and applications. *Advanced Functional Materials*, *28*(47), 1804950.